Vacancy analysis in a Ni-Nb-Zr-H glassy alloy by positron annihilation spectroscopy

doi: 10.1063/1.3688303

Vacancy analysis in a Ni-Nb-Zr-H glassy alloy by positron annihilation spectroscopy

Mikio Fukuhara

Citation: Applied Physics Letters **100**, 093102 (2012); doi: 10.1063/1.3688303
View online: http://dx.doi.org/10.1063/1.3688303
View Table of Contents: http://scitation.aip.org/content/aip/journal/apl/100/9?ver=pdfcov
Published by the AIP Publishing

Vacancy analysis in a Ni-Nb-Zr-H glassy alloy by positron annihilation spectroscopy

Mikio Fukuhara[a)]
Institute for Materials Research, Tohoku University, Sendai 980-8577, Japan

(Received 3 November 2011; accepted 7 February 2012; published online 27 February 2012)

The positron lifetimes of $Ni_{36}Nb_{24}Zr_{40}$ and $(Ni_{0.36}Nb_{0.24}Zr_{0.40})_{90}H_{10}$ glassy alloys are almost the same but longer than those of pure Zr, Nb, and Ni crystals, indicating that they have higher density of vacancies with smaller size than in crystals. The coincidence Doppler broadening spectrum for both specimens shows that the contribution of Ni around the vacancies is lower than that of Zr and Nb, suggesting that hydrogen atoms favour to exist between Ni atoms comprising neighboring distorted icosahedral $Zr_5Ni_5Nb_3$ clusters. Thus, these results provide a substitute model of quantum dot tunneling along Ni–H–Ni atomic bond arrays among the clusters. © *2012 American Institute of Physics*. [http://dx.doi.org/10.1063/1.3688303]

Quantum dot tunneling is currently attracting considerable attention in the field of physics.[1–6] We observed electric current-induced voltage oscillations in $\{(Ni_{0.6}Nb_{0.4})_{1-x}Zr_x\}_{100-y}H_y$ $(0.3 \le x \le 0.5,\ 0 \le y \le 20)$[7–9] and $\{(Ni_{0.6}Nb_{0.4})_{1-s}Zr_s\}_{100-z}D_z$ $(s = 0.30, 0.35, 0.40,$ and $0.45,\ 9.1 \le z \le 14.8)$[10] glassy alloys with multiple junctions in the temperature range 373-6 K on the basis of Coulombic oscillations of protons (deuteron). Based on the x-ray absorption fine structure (XAFS) atomic bonding data,[11] x-ray absorption near edge structure (XANES)[12] using strong radiation photons at SPring-8, and a Nyquist diagram (Cole-Cole plot) by ac impedance analysis using LCR meter,[13] we proposed that the quantum dot tunneling refers to charging and discharging of vacancy capacitance (0.9 fF)[8] of Zr(Nb)-H-□-H-Zr(Nb) atomic bond arrays among the electric-conducting distorted icosahedral $Zr_5Ni_5Nb_3$ clusters (dots of ~0.55 nm in size[14]), where □ is the vacancy tunnel in the glassy alloys. In particular, as the hydrogen content increases, the hydrogen atoms first penetrate into the space sites among the clusters and then construct zigzag tunnels of 0.26 nm average width[13] because of the high pressure effect of hydrogen in electrolysis.[15] In other words, the hydrogenized glassy alloy has a simple electric circuit with a resistor in parallel and a capacitor consisting of a large number of dielectric tunnels formed by hydrogen penetration. Thus, the glassy alloy of interest can be regarded as a dc/ac converting device with a large number of nanocapacitors with femtofarad capacitance.[15] However, since the location of hydrogen atoms is biased to approach Zr and Nb atoms comprising tetrahedrons in the clusters,[14] the tunneling path is not clear yet, although we have proposed it in previous papers.[7–10] Therefore, we consider a substitute model of quantum dot tunneling based on positron annihilation spectroscopy.

Here we note that glassy alloys are characterized by an assembly of vacancies that occupy between 0.7% and 3% of the total volume.[14] The number of such vacancies varies as the doping with hydrogen increases. Since it is important to investigate the distribution state of vacancy-like defects[16] in glassy alloys for understanding the mechanism behind the quantum dot tunneling, we determine the positron lifetime of a glassy alloy consisting of subnanometer-sized clusters. On the basis of Coulomb oscillation,[7–10,15] ballistic transport,[17,18] and large capacitance,[13] the results predict that glassy alloys are candidate materials for future nanometer size-electronic devices.

The goal here lies in studying vacancy distribution in alloys with and without hydrogen by using low-energy-positron annihilation analysis at room temperature. Positron annihilation, which is characterized by the emission of two γ-ray photons of 511 keV, provides detailed information about lattice defects such as vacancies, voids,[19] and dislocations. Coincidence Doppler broadening (CDB) of annihilation radiation also gives important information about electron density, electronic momentum density, etc.[19] The electron momentum distribution becomes narrower when positrons are trapped by defects in a material.[20,21] However, there is no previous research on the positron lifetime of Ni-Nb-Zr-H glassy alloys with femtofarad capacitance.

The amorphous $Ni_{36}Nb_{24}Zr_{40}$ alloy ribbons of about 1-mm width and 30 -μm thickness were synthesized from argon arc-melted ingots using free-jet melt spinning in Ar at a rotating speed of 3500 rpm (36.7 m/s). Hydrogen charging was carried out electrolytically in 0.5 M H_2SO_4 and 1.4 g/L thiourea (H_2NCSNH_2) at room temperature and at current densities of 30 A/m^2.[7–9,11–15] The amounts of hydrogen absorbed in the specimens were measured by the inert gas carrier melting-thermal conductivity method. The specimen density was measured using Archimedes's principle by weighing specimens in tetrabromoethane (density: 2.962 Mg/m^3) and air. The total free volumes before and after hydrogenation were 2.47% and 1.47%, respectively.

The structures of $Ni_{36}Nb_{24}Zr_{40}$ and $(Ni_{0.36}Nb_{0.24}Zr_{0.40})_{90}H_{10}$ glassy alloys were identified by x-ray diffraction using Cu Kα radiation in the grazing incident mode. The angle of incidence used was 2°.[22]

Positron lifetime measurements were carried out using a conventional fast-fast spectrometer with a time resolution of 190 ps at full width at half maximum (FWHM). About 4×10^6 coincidence events were accumulated for each time spectrum.

[a)]Electronic mail: fukuhara@imr.tohoku.ac.jp.

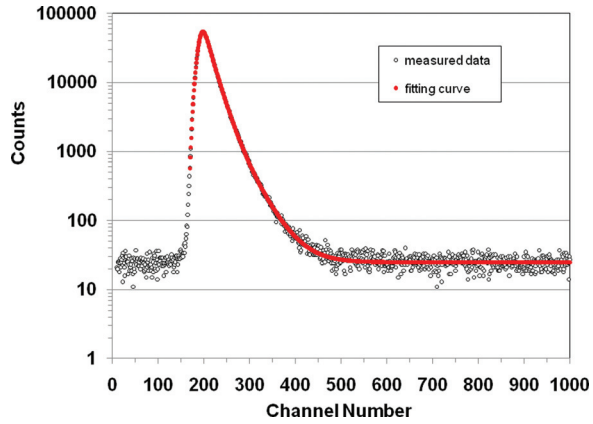

FIG. 1. (Color) Lifetime spectra for $Ni_{36}Nb_{24}Zr_{40}$ glassy alloy. Red line represents the fitting curve.

The CDB momentum distribution electron–positron annihilating pairs were obtained using two Ge detectors in coincidence. The coincidence measurement gives a background lower than that in a one-detector set-up by three orders of magnitude, which enables the measurement of the momentum distribution of the core electrons specific to each element, i.e., the high-momentum region.[23–25] The sample-detector distance was 20 cm. More than 2×10^7 total counts were accumulated in each measurement for 12 h. The overall momentum resolution was about 4.3×10^{-3} m_0c, where m_0 is the electron rest mass and c is the speed of light. The details of the setup are described in Refs. 24–26. The CDB ratio curves were obtained by normalizing the momentum distribution of each spectrum to that of the reference samples of well-annealed (defect-free) pure Zr, Nb, and Ni crystals. The shape of the ratio curves in the high-momentum region (typically $> 10 \times 10^{-3}$ m_0c) exhibits the characteristic broad peaks or valleys due to positron annihilation with Ni, Nb, and Zr core electrons. The low-momentum component fraction (LMCF) and high-momentum component fraction (HMCF) are defined as the ratios of the counts in low-momentum ($|p_L| < 4 \times 10^{-3}$ m_0c) and high-momentum (18×10^{-3} $m_0c < |p_L| < 30 \times 10^{-3}$ m_0c) regions in the CDB distributions to the total counts, respectively. It is well-known that the HMCF and LMCF are very sensitive to open-volumes. When the positrons are trapped by vacancy-type defects, the localized positrons have much higher probability of annihilation with the spread-out valence electrons from the surrounding atoms; therefore, the HMCF decreases and LMCF increases.[23–25] Furthermore, HMCF strongly reflects the chemical environment of the trapping site of positrons through their annihilation with the core electrons.

TABLE I. Positron annihilation lifetimes of $Ni_{36}Nb_{24}Zr_{40}$ and $(Ni_{0.36}Nb_{0.24}Zr_{0.40})_{90}H_{10}$ glassy alloys, and pure Zr, Nb, and Ni crystals.

Sample	Positron lifetime (ps)
$Ni_{36}Nb_{24}Zr_{40}$	172.1 ± 0.3
$(Ni_{0.36}Nb_{0.24}Zr_{0.40})_{90}H_{10}$	172.8 ± 0.3
Pure Ni	102.1 ± 0.3
Pure Nb	130.9 ± 0.3
Pure Zr	165.5 ± 0.3

Since all the positrons can be captured into mono-vacancies in bulk metals with total free volume over 10^{-4},[26] one can evaluate the positron annihilation technique to analyze the vacancies in a Ni-Nb-Zr glassy alloy with total free volume of 2.57%. The lifetime spectrum for the representative $Ni_{0.36}Nb_{0.24}Zr_{0.40}$ glassy alloy is shown in Fig. 1. All the positron lifetime spectra were best fitted to one experimental component.[24] The long-lived τ_2 component can be attributed to positron annihilation in the lower electron density region, e.g., defects. In general, the positron lifetime value provides information about not only the open pore volume size of vacancy-type defects but also their concentration. The lifetimes of the samples with H and without H are presented in Table I, along with those of the pure Ni, Nb, and Zr crystals. The lifetimes of the two specimens are almost the same as the values that we often observe in glassy alloys[27–29] but are longer than those of the three Zr, Nb, and Ni crystals. In comparison with the experimental positron lifetimes of 109, 120, and 164 ps for the bulk state and 180, 210, and 252 ps for the mono-vacancy state in Ni, Nb, and Zr crystals, respectively,[30] both alloys have higher density of vacancies with smaller size than the thermally activated mono-vacancies.[31] The long- and narrow-sized vacancies are characteristic of amorphous alloys.[27–29] Here we also note the special characteristics of how the positron wards off electric collision with hydrogen atoms. The same lifetime of both alloys suggests that hydrogen atoms do not exist in the vacancy sites among clusters. This leads to the assumption that hydrogen atoms penetrate and lie between Ni atoms in neighboring clusters and then enlarge the space because of the high-pressure effect of hydrogen in electrolysis. We have already reported that hydrogen exists among clusters in low hydrogen concentrations and penetrates the clusters as hydrogen concentration increases, on the basis of the calculated adiabatic potential energy of hydrogen atoms in the distorted icosahedral $Zr_5Ni_5Nb_3$ cluster.[17] Next, we focus on the Ni atom fraction around the vacancy in both alloys and the results of the CDB ratio analysis because the

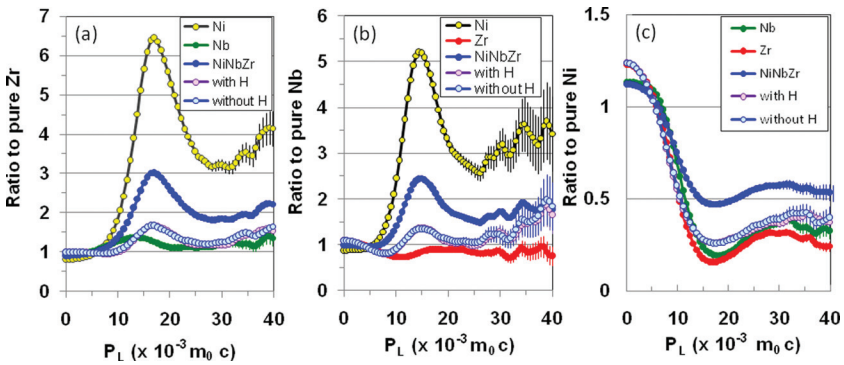

FIG. 2. (Color) Coincidence Doppler broadening ratio spectra of $Ni_{36}Nb_{24}Zr_{40}$ and $(Ni_{0.36}Nb_{0.24}Zr_{0.40})_{90}H_{10}$ glassy alloys, with those of Zr, Nb, and Ni metals, (a) ratio to pure Zr, (b) ratio to pure Nb, and (c) ratio to pure Ni.

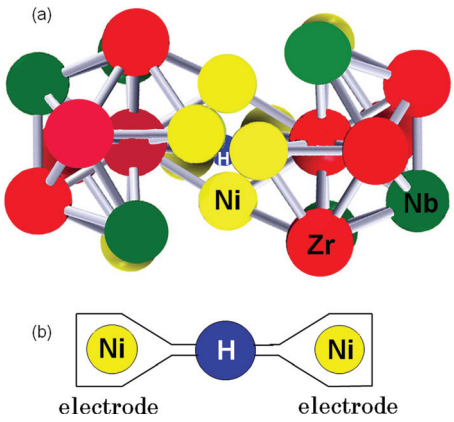

FIG. 3. (Color) Configuration pattern of two icosahedral clusters (a) and Coulomb dot tunneling model (b).

CDB can help distinguish the chemical element whose electrons annihilate the positron.[24]

Figure 2 shows the CDB ratio curves of both alloys and those of three pure Zr, Nb, and Ni crystals, expressed as ratios of CDB intensity of Zr (a), Nb (b), and Ni (c). The CDB spectrum for the H-free sample is nearly the same as that for the H-doped one. This means that the electronic momentum distribution around vacancies is almost the same in both alloys. The positron affinities of A− for Zr, Nb, and Ni are −3.98, −2.93, and −4.46 eV, respectively.[32] Since the differences in the positron affinity ΔA+ among $A+^{Zr}$, $A+^{Nb}$, and $A+^{Ni}$ are not so large, all elements might be attracted to the positron. Although the positron affinity for Ni is higher than that for Zr and Nb, the CDB ratio curve of Ni is remarkably large compared with those of Zr and Nb. On the other hand, the Zr, Nb, and Ni spectra for the chemical composition $Ni_{36}Nb_{24}Zr_{40}$ show lower contribution of Ni compared with Zr and Nb, indicating lower concentration of Ni for this chemical composition around vacancy sites. Judging from the above-mentioned results, Ni atoms tend to avoid vacancies in this alloy. In other words, hydrogen atoms prefer to exist among Ni atoms. Gupta[33] and Yukawa *et al.*[34] have reported that hydrogen in $LaNi_5$ hybridizes with Ni because of the energy states decreasing below the Fermi energy level, even though Ni has much lower affinity for H. Therefore, these results suggest a special cluster arrangement in which two Ni atoms belonging to each cluster approach each other or connect (Fig. 3(a)). Recent neutron scattering result also demonstrated the elongation of the Ni-Ni atomic distance by deuterium in a Ni-Nb-Zr-D glassy alloy.[35]

Judging from the above-mentioned results, we must revise the proposed model of quantum dot tunneling based on the Zr(Nb)-H-□-H-Zr(Nb) to Ni-H-Ni atomic bond arrays among the clusters. Figure 3(b) is a schematic representation of the microscopic junction between the distorted icosahedral $Zr_5Ni_5Nb_3$ clusters. This study provides new insight into the electron transport mechanisms such as Coulomb oscillation[7–10,15] and ballistic transport[17,18] at room temperature. Nonetheless, further work is needed.

We thank Emeritus Professor Dr. M. Hasegawa and Dr. T. Toyama (Tohoku University, Institute for Materials Research) for their helpful experiment and discussions. This study was supported by a Grant-In-Aid for Science Research in a Priority Area "Advanced Materials Development and Integration of Novel Structured Metallic and Inorganic Materials" from the Ministry of Education, Science, Sports.

[1]M. A. Kastner, P. F. Kwasnick, and J. C. Licini, Phys. Rev. B. **36**, 8015 (1987).
[2]T. A. Fulton and G. J. Dolan, Phys. Rev. Lett. **59**, 109 (1987).
[3]K. Ono, H. Shimada, and Y. Ootuka, J. Phys. Soc. Jpn. **67**, 2852 (1998).
[4]M. Stopa, Phys. Rev. Lett. **88**, 146802 (2002).
[5]K. M. Birnbaum, A. Boca, R. Miller, A. D. Boozer, T. E. Northum, and H. J. Kimble, Nature **436**, 87 (2005).
[6]E. Ben-Jacob and Y. Grefen, Phys. Lett. A **108**, 289 (1985).
[7]M. Fukuhara, A. Kawashima. S. Yamaura, and A. Inoue, Appl. Phys. Lett. **90**, 203111 (2007).
[8]M. Fukuhara, S. Yamaura, and A. Inoue, J. Phys. Conf. Ser. **144**, 012086 (2009).
[9]M. Fukuhara and A. Inoue, J. Appl. Phys. **105**, 063715 (2009).
[10]M. Fukuhara and A. Inoue, Europhys. Lett. **83**, 36002 (2008).
[11]H. Oji, K. Handa, J. Ide, T. Honma, S. Yamaura, A. Inoue, N. Umesaki, S. Emura, and M. Fukuhara, J. Appl. Phys. **105**, 113527 (2009).
[12]H. Oji, K. Handa, J. Ide, T. Honma, N. Umesaki, S. Yamaura, M. Fukuhara, A. Inoue, and S. Emura, J. Phys.: Conf. Ser. **190**, 012075 (2009).
[13]M. Fukuhara, M. Seto, and A. Inoue, Appl. Phys. Lett. **96**, 043103 (2010).
[14]M. Fukuhara, N. Fujima, H. Oji, A. Inoue, and S. Emura, J. Alloy Comp. **497**, 182 (2010).
[15]M. Fukuhara and A. Inoue, J. Appl. Phys. **107**, 033703 (2010).
[16]G. Kögel and W. Triftschäuser, in *Proceedings of 6th International Conference on Positron Annihilation*, edited by P. G. Coleman, S. C. Sharma, and L. M. Diana (University of Texas at Arlington, 1982), p. 595.
[17]M. Fukuhara and A. Inoue, J. Appl. Phys. **107**, 033703 (2010).
[18]M. Fukuhara, "Rotating speed effect on electronic transport behaviors of Ni-Nb-Zr-H glassy alloys," J. Alloy Comp. (in press).
[19]K. M. Flores, D. Suh, R. H. Dauskardt, P. Aska-Kumar, P. A. Strene, and R. H. Howell, J. Mater. Res. **17**, 1153 (2002).
[20]S. J. Wang, Z. Tang, Z. Q. Chen, Z. Y. Wu, and L. Ma, Physica C, **235–240**, 1219 (1994).
[21]C. Hidalgo and N. de Diego, Appl. Phys. A **27**, 149 (1982).
[22]M. Fukuhara, X. Wang, and A. Inoue, J. Non-Cryst. Sol. **356**, 1707 (2010).
[23]R. Krause-Rehberg and H. S. Leipner, *Positron Annihilation in Semiconductors*, Springer, Berlin, Heidelberg, 1999).
[24]Y. Nagai, M. Hasegawa, Z. Tang, Z. A. Hempel, K. Yubuta, T. Shimamura, Y. Kawazoe, A. Kawai, and A. Kano, Phys. Rev. B **61**, 6574 (2000).
[25]Y. Nagai, K. Takadate, Z. Tang, H. Ohkubo, H. Sunaga, H. Takizawa, and M. Hasegawa, Phys. Rev. B **67**, 224202 (2003).
[26]T. Toyama, Y. Nagai, Z. Tang, M. Hasegawa, A. Almazouzi, E. van Walle, and R. Gerard, Acta Mater. **55**, 6852 (2007).
[27]A. Ishi, A. Iwase, Y. Yokoyama, T. J. Konno, Y. Kawasuso, A. Yabuuchi, M. Maekawa, and F. Hori, J. Phys. Conf. Ser. **225**, 012020 (2010).
[28]R. Ditter, R. Wüschum, W. Ulfert, H. Kornmüller, and H.-E. Schaefer, Solid State Comm. **105**, 221 (1998).
[29]P. Asoka-Kumar, J. Hartley, R. Howell, P. A. Sterne, and T. G. Nieh, Appl. Phys. Lett. **77**, 1973 (2000).
[30]J. M. Campillo Robles, E. Ogando, and F. Plazaola, J. Phys.: Condens. Matter **19**, 176222 (2007).
[31]K. G. Lynn, C. L. Snead, Jr., and J. J. Hurst, in *Proceedings of 5th International Conference on Positron Annihilation*, edited by R. Hashiguchi and K. Fujiwara (The Japan Inst. Metal, 1979), p. 119.
[32]M. J. Puska, P. Lanki, and R. M. Nieminen, J. Phys. Condens. Matter **1**, 6081 (1989).
[33]M. Gupta, J. Alloy Comp. **293–295**, 120 (1999).
[34]H. Yukawa, T. Matsumura, and M. Morinaga, J. Alloy Comp. **293–295**, 227 (1999).
[35]T. Sato, D. Louca, K. Oyama, A. Llobet, M. Fukuhara, S. Iikubo, and K. Yamada, "Deuterium sites in glassy alloy $(Ni_{36}Nb_{24}Zr_{40})_{0.85}D_{0.15}$ studied by total neutron scattering combined with a reverse Monte Carlo simulation," J. Non-Cryst. Solids (submitted).